IL NUOVO CIMENTO **47 C** (2024) 74
DOI 10.1393/ncc/i2024-24074-3

Colloquia: IFAE 2023

The first year of the IXPE mission: A view on extended sources(*)

S. Silvestri
INFN, Sezione di Pisa - Pisa, Italy

received 13 February 2024

Summary. — Launched in December 9, 2021 as a SMEX (Small Explorer) NASA mission, IXPE (Imaging X-ray Polarimetry Explorer) is the result of a NASA/ASI joint effort to build the first telescope with space-resolved spectro-polarimetric capabilities in the soft X-ray band. In its first year of activity, IXPE successfully sampled tens of diverse sources, sometimes giving rise to quite unexpected results. In this contribution we briefly summarize the characteristics of the mission and its main results for selected extended sources that fully exploit IXPE's potential.

1. – Introduction

Polarimetry has been a tool in the hands of astronomers for more than a century now, providing much more information than flux alone. However, the exploitation of polarization properties has been possible only on selected energy bands, with the highest energy regimes being restricted to a handful of sparse measurements, insufficient to claim a systematic exploitation of polarimetry. First of its kind, IXPE is capable of space-resolved spectro-polarimetry and is designed to carry out a systematic survey of the X-ray sky (2–8 keV), and in the first year it has already observed multiple sources of several classes with dedicated observational campaigns. Given the diversity of IXPE's targets, only the results for extended sources are presented. The driver for this selections are the full exploitation of the power of space-resolved polarimetry and the common underlying astrophysical processes which make it convenient to summarize.

2. – The Imaging X-ray Polarimetry Explorer

IXPE consists of three identical X-ray mirror units focusing on three identical detector units. The mirror units are concentric shells in Wolter-1 configuration, and by focusing X-rays on a gas pixel detector (GPD, [1]) 4 meters apart, they achieve a peak effective area of 79.4cm^2 at 2.25 keV and a field of view of 11 arcminutes. The GPD is the hearth of the instrument and the real innovative part. The detection principle is based on photoelectric absorption happening in a sealed gas cell: upon being hit by an X-ray

(*) IFAE 2023 - "Cosmology and Astroparticles" session

the gas emits a photo-electron whose direction is preferentially aligned with the electric field of the incident photon, following the differential cross section

$$\frac{d\sigma}{d\omega} \sim Z^5 E^{\frac{7}{2}} \frac{\sin^2\theta\cos^2\phi}{(1+\beta\cos\theta)^4}, \tag{1}$$

where ϕ is the angle between the electric field and the emission direction on the plane of the detector. Each photoelectron initiates a cascade generating a track that is drifted by a drift field, amplified it with a gas electron multiplier, and read out and imaged. Upon reconstruction with a dedicated algorithm, we then get the event-by-event electric vector polarization angle which allows us to recover the polarization of the photon sample. The detection of polarization is clearer for longer tracks, generated by higher energy photons. The requirements of long tracks is what makes it important to have a gas instead of a solid where the range of the electrons would be too small to allow for clear detection. Even in our specifically optimized GPD, the length of a track is typically shorter than a millimeter (declining at lower energies) and smeared by diffusion. This makes it impossible to read polarization under 2 keV, where the tracks become essentially circular and the efficiency of the reconstruction algorithm drops. The observation of extended sources in IXPE is mostly affected by these limitations:

- Polarization leakage [2], a spurious effect of the reconstruction algorithm which happens on sharp and bright sources
- A spurious modulation from the manufacturing of the amplification stage of the GPD [1], which is averaged out through dithering
- Instrumental background [3] from both charged particles and secondary X-rays produced by particles that hit the detector. The effect of astrophysical background is negligible in all non-pathological cases (*e.g.*, when we are looking at a source embedded into another one)
- Charging, which is known to affect all gas electron multipliers and makes the gain of our final stage rate-dependent. This is more important for bright sources.

.

3. – The IXPE view of supernova Remnants

Supernova remnants are the outcomes of a stellar explosions. Such explosions happen in an environment which is the result of the history of the stellar activity of both the progenitor and neighbouring stars. As such, it is supposed to be composed by a magnetized plasma whose conditions vary from one object to another. As the explosion happens, a shock front departs from the progenitor, energizing the surroundings and ionizing neutrals.Subsequent cooling leads to recombination in a much longer time scale since the mean free path is usually quite large and the matter cools slowly and out of equilibrium. The plasma mixture of ions and electrons spiral in the local magnetic field, emitting synchrotron radiation with a typical broad band power-law spectrum that extends from radio waves up to X-rays. The spectral properties of observed photons depend on the seed electrons' energy, so that when we look at X-ray photons we expect an electron population at TeV energies being responsible for such emission, whereas at lower energy we are looking at a population of lower energy particles. When looked at in

radio waves, supernova remnants typically show spatial features that are much broader than when looked at in X-rays, and quite often the radio shell is contained in the X-ray shell: both of these characteristics are clear tracers of the evolution of the plasma, which shines in the X-ray when promptly accelerated and fades away as it cools down, lighting up in radio waves further downstream of the shock as the magnetic field burns its energy off through synchrotron The lifetime spent in radiating above a given energy has been estimated to be [4]

$$\tau_{\rm synch} \sim 12.5 \left(\frac{B}{100\mu G}\right)^{-2} \left(\frac{E_e}{100{\rm TeV}}\right)^{-1} {\rm yr}, \tag{2}$$

where E_e is the energy of the radiating electrons, so that higher energy radiation is expected to manifest in thinner features, as for a radially expanding shock fronts time can be mapped in space through the shock velocity. On the other hand, polarization degree and angle give information about the status of the magnetic field that the electron population is radiating in, with the (average) polarization direction being orthogonal to the (average) magnetic field direction and the polarization degree representing the coherence of the magnetic field for the photon sample of interest (*i.e.*, pixel size and time interval). Seeing X-ray synchrotron photons is already an important clue for SNRs being accelerators likely to be responsible of the comic ray spectrum observed at the earth, but with polarization we can infer the properties of the magnetic field right at the acceleration sites, and not further downstream as for the case of radio waves, possibly ruling out some mechanisms.

3˙1. *Radio vs. X-ray band polarimetry: what have we learnt.* – In its first year, IXPE has observed three historical SNR: Cas A, Tycho's SNR and SN1006, for which radio observations already existed. In radio band, all young (*e.g.*, $<$ few kyr) SNR show a radial magnetic field with a high degree of turbulence, which is in contrast with the simplest MHD expectations unless one thinks of selection issues or instabilities developing only on young SNR. Such instabilities, however, might develop either at the shock front or in the pre-shock region or downstream the shock, but radio polarimetry alone is insufficient to answer this question. The results from IXPE observation of historical supernova remnants have so far been aligned to those in radio waves, and due to SNR being relatively smooth and diluted no correction due to polarization leakage has been necessary. Cas A [5], our first sample, could reach the required sensitivity to claim a certain detection only by integrating all of the signal in the external shell. The procedure was one that became a standard for the next SNR works: a simulation based on Chandra X-ray observations provided a map of the amount of synchrotron and thermal component, and we added our best knowledge of IXPE internal background to estimate the dilution and infer the optimal energy band for polarization detection. In this case, only a weak polarization signal existed, so we required to have the largest possible counts to make it significant, thus the integration. The recovered polarization angle is compatible with the highest energy particle's emission happening in a radially aligned magnetic field, with a lower than in radio band polarization degree. However, we warn the reader that integration over progressively larger areas is known to wash out the polarization degree, so in this case the lower polarization degree is not supposed to indicate an intrinsically more turbulent magnetic field. The other samples were bright and polarized enough to provide a map of polarization, fully exploiting IXPE's capabilities: Tycho's SNR [6] exhibits a radially aligned magnetic field again, but this time the polarization degree was

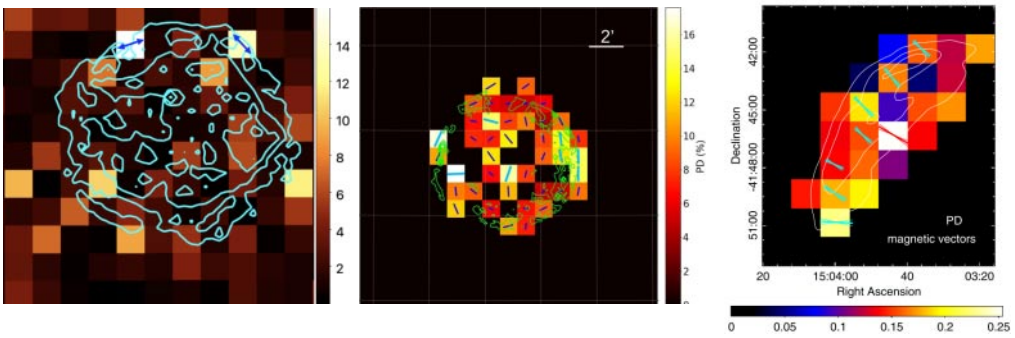

Fig. 1. – Polarization maps for our first year supernova remnant sample from [5-7]. On the left panel, Cas A χ^2 map 2d histogram with intensity contours from Chandra superimposed and arrows representing the polarization direction (orthogonal to magnetic field) for significant ($> 3\sigma$)bins. In the middle panel, polarization degree map of Tycho's SNR with polarization vectors superimposed. The color of the vectors represent the significance, with thicker bars representing $> 2\sigma$ detections, and the length of the bar representing the polarization degree. On the right, the map of the northeastern rim of SN1006 with magnetic field vectors superimposed to the significance map (blue and red represent $> 2\sigma$ and $> 3\sigma$ respectively)

higher than in radio waves (12% on average, up to 23%) against 8%, and an analysis of SN1006 data [7] again revealed a similar scenario with a radially aligned magnetic field and an even higher polarization degree of 24% on average. While the complete picture has not emerged yet (and private communications suggest a completely different scenario for IXPE's 2023 SNR sample), it is the first time that we probe the magnetic field structure at the acceleration site of SNR and we can already draw some conclusions. It seems plausible that the the ambient could play a key role on the turbulence and orientation of the magnetic field (see the discussion on [7]). While the radial magnetic fields in SNR are not well understood yet (even after years of radio observations), one of the most frequently cited mechanism for radial magnetic fields are MHD instabilities at the shock front (An impulsive version of the usual Rayleigh-Taylor instability, named after Richtmyer and Meshkov, see [8] for a compared overview on the two). Such instabilities are known to grow mostly on clumpy media and are less likely on cloudy media. Moreover, the density influences also the characteristic scale of turbulence. In these scenario, clumpy media favor radial magnetic field structure and low density favors higher polarization degree, which aligns well with IXPE findings on historical SNR.

4. – The IXPE view of Pulsar Wind Nebulae

Pulsar wind nebulae (PWN) share a common origin with supernova remnants as they are both what's left of a stellar explosion. The same considerations about the environment apply, but this time we are not looking at the outskirt of the expanding shock front, but rather on the activity of the central strongly magnetized neutron star that formed as a remnant, named pulsar. PWN are still to be completely understood but a common although very simplified explanation for their emission is that of charged particles launched from the stellar surface co-rotating with the magnetic field of the pulsar which is misaligned with respect to the spinning axis. Since the pulsar is rapidly spinning, there will be some radius after which the tangential speed will exceed the speed

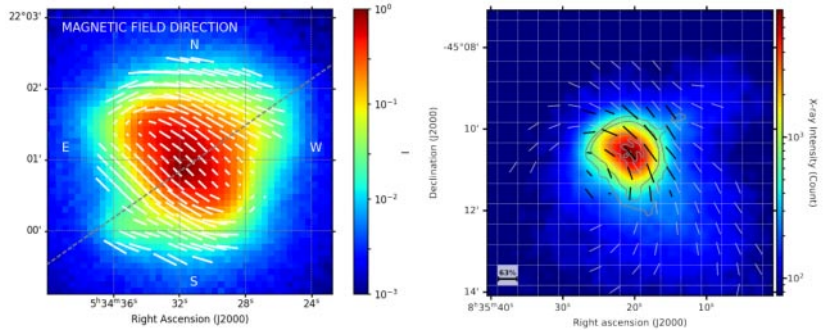

Fig. 2. – Polarization maps for the Crab (left, from [10]) and Vela (right, from [11]) PWN. For the Crab, all white bars superimposed to the intensity profile represent the average magnetic field computed in a fine-binned smoothed map with a kernel about the size of IXPE's PSF (see [10] for details). A 5 σ significance cut has been applied, so each bar is a significant detection. For the Vela PWN no smoothing has been applied and a coarse binning has been preferred. The white bars represent the radio polarization at 5 GHz and the black bars the X-ray polarization. Gray contours are derived from Chandra to better highlight the PWN structure.

of light, and the co-rotation will then be impossible, the field lines will open up and an outflowing, high relativistic and strongly magnetized wind of particles will form. At a much larger radius, this wind is supposed to convert its magnetic to particle energy after hitting some kind of boundary, forming the pulsar wind nebula. A very thorough bibliography and introductory explanation on the subject is contained in [9]. By looking at the polarization properties of the emission of PWN, IXPE aims at contributing to understand the energy conversion mechanism happening at such boundary.

4˙1. *X-ray emission and polarization of PWN.* – X-ray emission of pulsar + PWN systems is present at the surface of the pulsar and then much further away, where it can be fitted with a typical broken power law spectrum. The sudden brightening of matter in X-ray at the is what motivates the argument of energy conversion. The shape implies a toroidal magnetic field configuration with particles radiating synchrotron, suggesting that some winding of the magnetic field lines happens away from the central object. The leading hypothesis in describing the underlying processes is that of particles hitting some kind of boundary (termination shock) upon which they convert their magnetic energy in particle energy and bright up. The exact mechanism for this energy conversion is still unknown, but the two major candidates are turbulent acceleration or reconnection. In first year's IXPE observations, none of these mechanisms have been ruled out. For the Crab PWN [10], a toroidal magnetic field structure has indeed been confirmed, and a high polarization degree also suggested a rather uniform magnetic field with little turbulence, but the patchy structure of the polarization degree, in contrast with a uniform luminosity profile, suggest that although the magnetic field is on average very coherent, the energization of particles is sustained also in turbulent domains that wash out the polarization. In contrast, IXPE observations of the Vela PWN [11] reveal once again a high polarization degree (in some regions up to the theoretical value of synchrotron from a perfectly uniform magnetic field), with a much higher uniformity across the whole PWN, indicating that magnetic reconnection is more likely to accelerate particles w.r.t. turbulence.

* * *

The Imaging X ray Polarimetry Explorer (IXPE) is a joint US and Italian mission. The US contribution is supported by the National Aeronautics and Space Administration (NASA) and led and managed by its Marshall Space Flight Center (MSFC), with industry partner Ball Aerospace (contract NNM15AA18C). The Italian contribution is supported by the Italian Space Agency (Agenzia Spaziale Italiana, ASI) through contract ASI-OHBI-2017-12-I.0, agreements ASI-INAF-2017-12-H0 and ASI-INFN-2017.13-H0, and its Space Science Data Center (SSDC) with agreements ASI-INAF-2022-14-HH.0 and ASI-INFN 2021-43-HH.0, and by the Istituto Nazionale di Astrofisica (INAF) and the Istituto Nazionale di Fisica Nucleare (INFN) in Italy. This research used data products provided by the IXPE Team (MSFC, SSDC, INAF, and INFN) and distributed with additional software tools by the High-Energy Astrophysics Science Archive Research Center (HEASARC), at NASA Goddard Space Flight Center (GSFC). The research at Guangxi University was supported in part by National Natural Science Foundation of China (Grant No.12133003). The research at Boston University was supported in part by National Science Foundation grant AST-2108622. I.A. acknowledges financial support from the Spanish "Ministerio de Ciencia e Innovación" (MCINN) through the "Center of Excellence Severo Ochoa" award for the Instituto de Astrofísica de Andalucía-CSIC (SEV-2017-0709) and through grants AYA2016-80889-P and PID2019-107847RB-C44.

REFERENCES

[1] Baldini L., Barbanera M., Bellazzini R., Bonino R., Borotto F. *et al.*, *Astropart. Phys.*, **133** (2021) 102628.
[2] Bucciantini N., Di Lalla N., Romani R. W. R., Silvestri S., Negro M. *et al.*, *Astron. Astrophys.*, **672** (2023) A66.
[3] Di Marco A., Soffitta P., Costa E., Ferrazzoli R., La Monaca F., Rankin J., Ratheesh A., Xie F., Baldini L., Del Monte E., Ehlert S. R., Fabiani S., Kim D. E., Muleri F., O'Dell S. L., Ramsey B. D., Rubini A., Sgrò C., Silvestri S., Tennant A. F. and Weisskopf M. C., *Astron. J.*, **165** (2023) 143.
[4] Vink J. and Zhou P., *Galaxies*, **6** (2018) 46.
[5] Vink J., Prokhorov D., Ferrazzoli R., Slane P., Zhou P. *et al.*, *Astrophys. J.*, **938** (2022) 40.
[6] Ferrazzoli R., Slane P., Prokhorov D., Zhou P., Vink J. *et al.*, *Astrophys. J.*, **945** (2023) 52.
[7] Zhou P., Prokhorov D., Ferrazzoli R., Yang Y.-J., Slane P. *et al.*, *Astrophys. J.*, **957** (2023) 55.
[8] Zhou Y., Williams R. J. R., Ramaprabhu P., Groom M., Thornber B. *et al.*, *Phys. D: Nonlinear Phenom.*, **423** (2021) 132838.
[9] Mitchell A. M. W. and Gelfand J., *Pulsar Wind Nebulae*, in *Handbook of X-ray and Gamma-ray Astrophysics* 2022, p. 61.
[10] Bucciantini N., Ferrazzoli R., Bachetti M., Rankin J., Di Lalla N. *et al.*, *Nat. Astron.*, **7** (2023) 602.
[11] Xie F., Di Marco A., La Monaca F., Liu K., Muleri F. *et al.*, *Nature*, **612** (2022) 658.